Influences of dynamic material properties of slab track components on the train-track vibration interactions

Li, Ting; Su, Qian; Kaewunruen, Sakdirat

DOI:
10.1016/j.engfailanal.2020.104633

Document Version
Peer reviewed version

Citation for published version (Harvard):
Li, T, Su, Q & Kaewunruen, S 2020, 'Influences of dynamic material properties of slab track components on the train-track vibration interactions', *Engineering Failure Analysis*, vol. 155, 104633.
https://doi.org/10.1016/j.engfailanal.2020.104633

Influences of dynamic material properties of slab track components on the train-track vibration interactions

Ting Li[a,b,c], Qian Su[a,b], Sakdirat Kaewunruen[c,*]

[a] *School of Civil Engineering, Southwest Jiaotong University, Chengdu 610031, China*

[b] *Key Laboratory of High-Speed Railway Engineering, Ministry of Education, Southwest Jiaotong University, Chengdu 610031, China*

[c] *School of Engineering, University of Birmingham, Birmingham B15 2TT, UK*

[*]Correspondence should be addressed to Sakdirat Kaewunruen (s.kaewunruen@bham.ac.uk).

Abstract: Slab tracks or so-called ballastless tracks have been widely adopted for highspeed rail networks. Material properties of slab track components have significant influences on the serviceability performance of both high-speed trains and the slab tracks. In reality, the stiffness of rail pads and moduli of elasticity of concrete and CA mortar are quite different when they are determined by using either quasi-static or dynamic loading tests. Based on a critical literature review, most previous studies adopted some static material properties despite the fact that the actual loads from high-speed trains onto slab tracks are dynamic excitation. In addition, some studies simply adopted the dynamic stiffness of rail pads whilst ignored the dynamic effect on modulus of elasticity in their simulations. This study is thus aimed at highlighting the influence of the dynamic material properties on the train-track vibration interactions. A nonlinear 3D coupled vehicle-slab track model has been developed based on the multi-body simulation principle and finite element theory using LS-DYNA. This model has been validated by comparing its results with field test data together with other simulation results. A good agreement among the results has been found. The magnification effect on the dynamic modulus of elasticity under dynamic train loads has been determined firstly. The influences of material properties on the serviceability performance of the vehicle, the wheel-rail contact force, the vibration responses of the rail, concrete slab, and CA mortar have then been evaluated. The deviation coefficients of vibration responses of the vehicle and track under three types of material properties have been determined to emphasise the influences of the dynamic stiffness and modulus of elasticity. The insight from this study provides a new

reference and recommendation for adopting suitable and realistic material properties of high-speed slab tracks in practice.

Keywords: dynamic material properties; strain-rate effect; train-track interactions; high-speed railway; finite element model

1. Introduction

Slab tracks have become a prevalent trend for highspeed railways throughout the world because of its advantages for higher stability, lower track deformation, and much lower maintenance compared with ballasted tracks [1, 2]. In China, the operating mileage of highspeed railway networks has reached 29,000 km by the end of 2018, and most of the track structures are indeed slab tracks [3, 4]. The China Railway Track System (CRTS) I slab track is a typical non-ballasted track structure, which has been adopted in many high-speed railways in China, such as Qinhuangdao-Shenyang passenger dedicated line, Shanghai-Nanjing intercity railway line, and Chengdu-Mianyang-Leshan High-speed railway line. This slab track is mainly composed of the CHN60 rail (Chinese standard rail with the rail mass 60 kg/m), the WJ-7B fastener system, the concrete slab, the cement-emulsified asphalt (CA) mortar layer, and the concrete base, as illustrated in Figure 1.

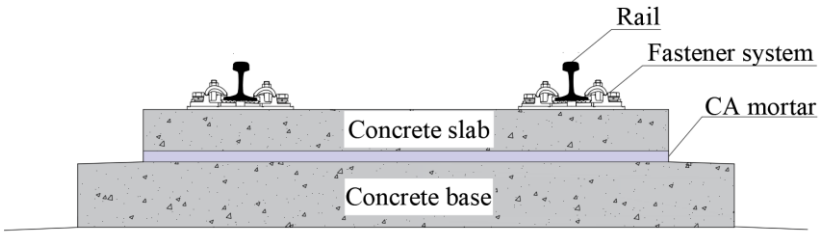

Figure 1 Section of the CRTS I slab track

Material properties of the slab track are an essential element for designing and predicting the dynamic performance of the high-speed railway under dynamic train loads. This dynamic performance is often the governing requirement as part of serviceability limit states for track systems. In practice, the elastic constitutive model of slab tracks is often used in design and numerical predictions. Material properties of track components are the key factors for the constitutive models, mainly consisting of the mass density, the modulus of elasticity, and the Poisson's ratio for solid elements, and the stiffness and damping for spring-dashpot elements.

In order to determine vehicle-track interactions, the designed static material properties of the slab track components are normally adopted in most previous studies and these properties are mainly measured from the quasi-static loading tests in laboratories [5-7]. For example, the modulus of elasticity of the concrete slab is 3.6×10^{10} Pa, which is determined by the compressive strength test for the C60 concrete, and the test loading is simply static [7]. The stiffness of the rail pads in WJ-7B fastener system is 2.5×10^{7} N/m, which is also measured from the static loading tests [7]. These material properties are the static properties obtained from benchmarking test requirements. In real life, a train will apparently impart dynamic excitations onto slab tracks. Especially when the train speed becomes faster, the vibration induced by the dynamic train loads will cause a lot of defects to track components [4, 8-10]. Thus, appropriate material properties of slab track components shall be taken into account when performing dynamic interaction simulations. Several studies have shown that the properties of various materials such as concrete and cement-based materials under dynamic loads will be magnified compared with the properties under static or quasi-static loads, especially for the modulus of elasticity [11-13]. For rails, it is a composite metal material with chemical elements like C, Mn, Si, P, S, and so on. The modulus of elasticity of rail is not sensitive to the dynamic excitation so that it will not change much under dynamic train loads [14]. However, it is well known that the concrete is a strain-rate dependent material under dynamic loads, indicating the modulus of elasticity of concrete will be increased significantly with strain rates [15-18]. The CA mortar is also sensitive to strain rates under dynamic loads [19-22]. Zeng et al. [23] carried out an experiment to study the dynamic properties of CA mortar in CRTS I slab track and the dynamic modulus of elasticity of CA mortar could be increased by 75% of the static values. As the main elastic elements to absorb the vibration energy, the soft rail pads are normally installed in high-speed railways [24, 25]. The static stiffness of rail pads is 20-30 kN/mm according to the design code of high-speed railways in China. However, the dynamic stiffness of rail pads is not easy to be determined because the rail pad is a frequency- and temperature- dependent material in practice [26]. Hopefully, the rail pads are normally simplified as the spring elements in numerical simulations and the constant values have been normally adopted [27]. The dynamic stiffness of rail pads under cyclic loads is around 1.3-2 times the static stiffness for WJ-7B fastener system [28, 29]. It is

noted that other material properties such as the mass density and the Poisson's ratio are not sensitive to the dynamic strain rates, whilst the damping must be determined by the dynamic loading tests [30]. Therefore, relatively among all of the elastic materials properties, the modulus of elasticity and the stiffness are the most sensitive properties to the dynamic excitations in slab tracks.

Dating back to 1978, Birmann [31] was the first to study the dynamic modulus of elasticity of the ballasted track with regard to high speeds through simulations. However, at that time, the train and track were just simplified using a multi-body simulation idealization as the mass and spring models due to the low computational efficiency, so the train-track vibration interactions like wheel-rail contact force and dynamic stress of the track components cannot be acquired. Nowadays, the 3D coupled vehicle-track numerical model has become an efficient solution to study the complicated dynamic performance of the high-speed railways [27, 32]. However, the static material properties of the slab track components are still adopted on a large scale in many numerical models [33-36]. For example, Zhu et al. [33, 34] developed a 3D coupled vehicle-track model to study the deterioration of the slab track by using static properties. Xu et al. [35] also used the static properties in the coupled vehicle-track model to analyze the stochastic vibrations. Sun et al. [36] analyzed the track-bridge vibration by using static properties of the slab tracks. In addition, some scholars like Zhai et al., Lei et al., and Ren et al., [37-39] combined the dynamic stiffness of rail pads with still static modulus of elasticity for concrete and CA mortar in their coupled vehicle-track models to analyse the dynamic performance, but nearly nobody explains why both static and dynamic material properties were used in the one simulation model under dynamic excitations. To the authors' knowledge, there are no previous studies investigating the influences of the dynamic material properties of slab track components on train-track vibration interactions. It is still questionable at large whether it is appropriate for predicting the dynamic performance of the railway by using static material properties and whether there is a need to consider fully the dynamic properties of slab track components in the coupled vehicle-track numerical models under actual dynamic train excitations.

In order to investigate the influences of the dynamic material properties of the slab track components on the vibration responses of the train and track, a nonlinear 3D coupled

115 vehicle-slab track numerical model has been developed based on the multi-body simulation
116 principle and finite element method using LS-DYNA. Three types of material properties of
117 slab track components have been adopted for the parametric studies: static stiffness for rail
118 pads and static modulus of elasticity for concrete and CA mortar, dynamic stiffness for rail
119 pads and static modulus of elasticity for concrete and CA mortar, and dynamic stiffness for
120 rail pads and dynamic modulus of elasticity for concrete and CA mortar. The 3D model has
121 been validated firstly. Then, the magnification effect of the dynamic modulus of elasticity has
122 been analyzed. Accordingly, the vibration of the vehicle, the wheel-rail contact force, the
123 vibration responses of the slab tracks can be determined for various train speeds from 10 km/h
124 to 400 km/h, taking into account the three types of material properties. Ultimately, the
125 deviation coefficients, which present the influence of the properties on vibration responses,
126 have been evaluated to provide the evidence and recommendation for adopting suitable and
127 realistic material properties of high-speed slab tracks in practice.

128 ## 2. Material properties of the slab track

129 The material properties of the slab track are different when they are measured by either
130 quasi-static or dynamic loading tests. When the properties are measured by quasi-static
131 loading tests, the material properties are named as static properties in this paper. In contrast,
132 when they are measured by dynamic loading tests, the properties are named as dynamic
133 properties. The static and dynamic material properties of CRTS I slab track are presented in
134 the following parts.

135 ### 2.1 Static properties of the slab track

136 The static material properties of the CRTS I slab track components can be found in [7],
137 as shown in Table 1. The stiffness of rail pads and the moduli of elasticity of the concrete slab,
138 CA mortar, and concrete base are determined from the quasi-static loading tests.

139 Table 1 Static properties of the CRTS I slab track

Properties	Values
Mass density of the rail (kg/m^3)	7830

Modulus of elasticity of the rail (Pa)	2.059×10^{11}
Poisson's ratio of the rail	0.3
Stiffness of the rail pads (N/m)	2.5×10^{7}
Damping of the rail pads (N.s/m)	7.5×10^{4}
Mass density of the concrete slab (kg/m^3)	2500
Modulus of elasticity of the concrete slab (Pa)	3.6×10^{10}
Poisson's ratio of the concrete slab	0.2
Mass density of the CA mortar (kg/m^3)	1600
Modulus of elasticity of the CA mortar (Pa)	3×10^{8}
Poisson's ratio of the CA mortar	0.2
Mass density of the concrete base (kg/m^3)	2500
Modulus of elasticity of the concrete base (Pa)	3.25×10^{10}
Poisson's ratio of the concrete base	0.2

2.2 Dynamic stiffness of the rail pads

The rail pads play an important role in reducing vibration on track components. They are normally made out of rubber, high-density polyethylene (HDPE), thermoplastic polyester elastomer (TPE), and ethylene vinyl acetate (EVA) [24, 25]. The rail pads also come in a wide range of stiffness due to different types of materials. So that the stiffness of rail pads can be classified as soft, medium, stiff, very stiff, and extremely stiff [25]. However, there are no standard classification values for the rail pads around the world since the properties vary in relation to track characteristics. According to [25], the stiffness of soft pads is less than 80 or 130 kN/mm, and the soft pads are normally used in WJ-7B fastener system, which is widely adopted in high-speed railways in China.

According to the literature reviewed, the dynamic stiffness of rail pads is temperature- and frequency-dependent, and it is also sensitive to the preloads when the stiffness is tested in the laboratory [24, 26, 40]. Therefore, the dynamic stiffness of rail pads is a complicated parameter in practice. Hopefully, in order to describe the viscoelasticity characteristics of rail pads, the rail pads are normally simplified as the spring and dashpot elements, so that the

constant values are normally used in the numerical simulation models to describe the dynamic characteristics of rail pads [27, 32].

When the constant value is used, the dynamic stiffness of rail pads is normally 1.3-2 times the static value according to previous studies [28, 29]. For the coupled vehicle-track model, many researchers used two times the static stiffness to represent the dynamic characteristics of rail pads [28, 37-39]. Since the static stiffness of rail pads in this paper is 25 kN/mm, the dynamic stiffness of rail pads is determined as 50 kN/mm for CRTS I slab track in this study, as shown in Table 2.

Table 2 Stiffness of the rail pads in CRTS I slab track

-	Static stiffness	Dynamic stiffness
Values (kN/mm)	25	50

2.3 Strain-rate-dependent moduli of elasticity of the concrete and CA mortar

The effect of strain-rate on modulus of elasticity for concrete under dynamic loads has been studied by many researchers [41, 42]. The Comite Euro-International Du Beton (CEB) has put forward the strain-rate enhancement factors for the compressive and tensile modulus of elasticity as follows [30]:

$$\eta_c = \frac{E_d}{E_s} = \left(\frac{\dot{e}}{\dot{e}_{sc}}\right)^{0.026} \tag{1}$$

$$\eta_t = \frac{E_d}{E_s} = \left(\frac{\dot{e}}{\dot{e}_{st}}\right)^{0.016} \tag{2}$$

Where η_c and η_t are the compressive and tensile strain-rate enhancement factors, respectively; E_d and E_s are the dynamic and static modulus of elasticity, respectively; $\dot{e}$ is the effective strain-rate of concrete under dynamic loads; $\dot{e}_{sc}$ is the effective strain-rate of concrete under compressive static loads, and it equals to 30×10^{-6} /s; and $\dot{e}_{st}$ is the effective strain-rate of concrete under tensile static loads, and it equals to 3×10^{-6} /s. Note that the relationship between the effective strain-rate and the strain-rate components in different directions can be calculated as follows:

$$\dot{e} = \sqrt{\frac{2}{3}\{\dot{\varepsilon}_{ij}\dot{\varepsilon}_{ij}\}}^{1/2} = \sqrt{\frac{2}{3}\{\dot{\varepsilon}_1^{\,2} + \dot{\varepsilon}_2^2 + \dot{\varepsilon}_3^2\}}^{1/2}$$
$$= \frac{2}{3}\{\frac{1}{2}[(\dot{\varepsilon}_x - \dot{\varepsilon}_y)^2 + (\dot{\varepsilon}_y - \dot{\varepsilon}_z)^2 + (\dot{\varepsilon}_z - \dot{\varepsilon}_x)^2] + \frac{3}{4}(\dot{\gamma}_{xy}^{\,2} + \dot{\gamma}_{yz}^{\,2} + \dot{\gamma}_{zx}^2)\}^{1/2} \quad (3)$$

Where $\dot{\varepsilon}_1, \dot{\varepsilon}_2$, and $\dot{\varepsilon}_3$ are the principal strain-rates; $\dot{\varepsilon}_x, \dot{\varepsilon}_y$, and $\dot{\varepsilon}_z$ are the normal strain-rates in three directions, and $\dot{\gamma}_{xy}, \dot{\gamma}_{yz}$, and $\dot{\gamma}_{zx}$ are the shear strain-rates in three directions.

It is quite difficult to determine which parts of the concrete slab and concrete base are under compressive- or tensile- state when the train passes by since the dominant mechanical state changes typically with time. By referring to the method for strain-rate enhancement in Winfrith concrete model [41, 42], the average strain-rate enhancement factor is used for concrete slab and concrete base:

$$\eta_{aver} = \frac{1}{2}(\eta_c + \eta_t) \quad (4)$$

The compressive-, tensile-, and average- enhancement factors are calculated with the effective strain-rate, as shown in Figure 2. When the strain-rate changes from 1×10^{-6} /s to 1 /s, the maximum deviation between compressive factor and tensile factor is around 7% at 1 /s, indicating that the average enhancement factor will not cause a significant deviation to the dynamic analysis. Note that the static effective strain-rates for compression and tension are 3×10^{-5} /s and 3×10^{-6} /s, respectively, when the effective strain-rate is lower than the static values, the enhancement factor is set to equal to 1. And the average static effective strain-rate is 1.65×10^{-5} /s.

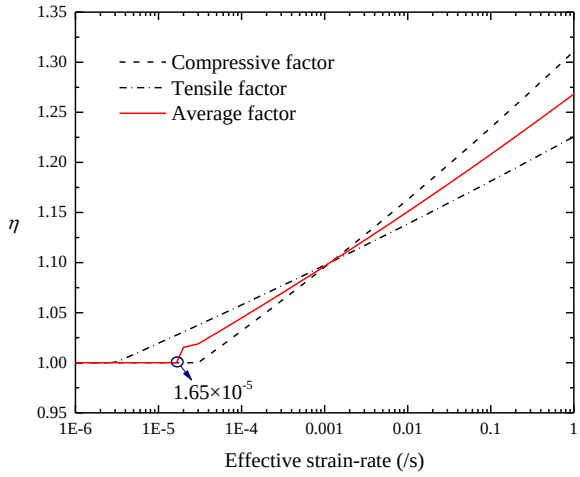

Figure 2 The strain-rate enhancement factors with effective strain-rate for concrete

According to [23], the strain-rate enhancement factor for modulus of elasticity of CA mortar in CRTS I slab track can be acquired from the tested values, as shown in Figure 3. The fitting curve is calculated as follows:

$$\eta = 2.01416 \times \dot{e}^{0.07836} \tag{5}$$

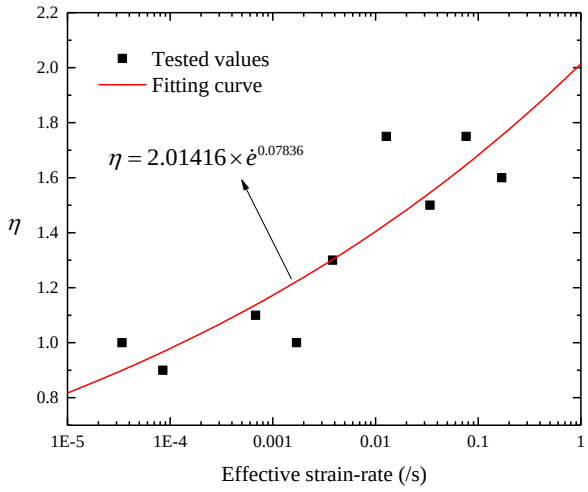

Figure 3 The strain-rate enhancement factor with effective strain-rate for CA mortar

3. Development of the numerical model

In order to investigate the influence of the dynamic material properties of the slab track on the vibration responses of the train and track, a 3D coupled vehicle-slab track numerical model has been developed, as shown in Figure 4. The vehicle is developed based on the multi-body simulation principle, and the slab track is simulated based on the finite element theory using the commercial software LS-DYNA.

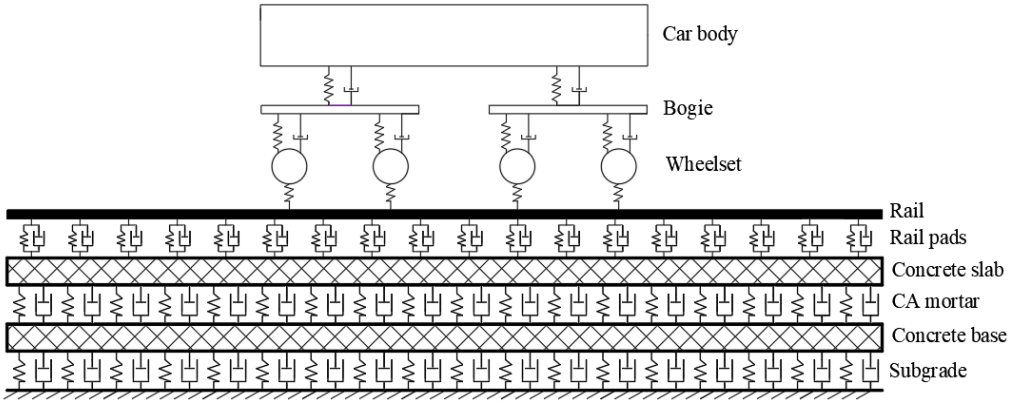

Figure 4 The coupled vehicle-slab track numerical model

3.1 Vehicle and slab track elements

The vehicle consists of one car body, two bogies, four wheelsets, and two-stage suspension system. The car body, bogies, and wheelsets are simplified as rigid bodies using shell and beam elements. Each component of the vehicle is connected by the suspension springs and dashpots. The vehicle has a total 10 degrees of freedom, including the vertical and pitch motion of the car body, vertical and pitch motion of the bogies, and vertical motion of the wheelsets. The slab track is composed of rail, rail pads, concrete slab, CA mortar, and concrete base. The rail is modeled as Euler beam supported by rail pads, which are simulated as the spring and dashpot elements. The concrete slab, CA mortar, and concrete base are modeled by solid elements in order to acquire the complicated 3D mechanical state. And the subgrade is described as the spring-damping system, which is widely used in many simulation models [27, 35]. The whole model has 38,344 elements including beam, shell, solid, spring, and dashpot, as shown in Figure 5.

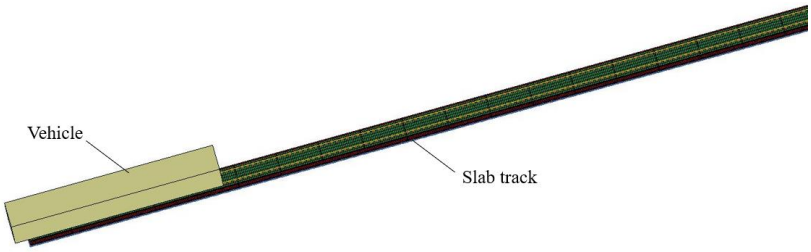

(a)

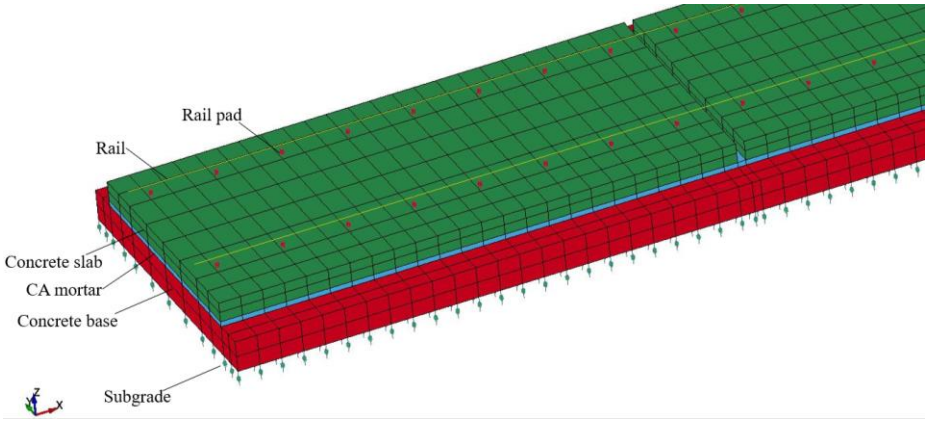

(b)

Figure 5 The coupled vehicle-slab track model in LS-DYNA (a) Top view of the entire model (b) Detailed slab track model

3.2 Wheel-rail contact theory

The wheel-rail contact is developed by the built-in keywords in LS-DYNA: *Rail_Track and *Rail_Train. Users can input the contact parameters like the stiffness of the wheel-rail contact spring, the irregularity of the track, and so on.

The wheel-rail contact force can be calculated automatically by LS-DYNA based on the following equation:

$$F = K \times (Z_w - Z_r - \delta) \tag{6}$$

Where F is the wheel-rail contact force; K is the vertical stiffness of the wheel-rail contact spring, K =1.325×10^9 N/m in this study [38]; Z_w is the vertical displacement of the wheel; Z_r is the vertical displacement of the rail; and δ is the track irregularity.

The irregularity of the Germany high-speed low disturbance is used to excite the wheel-rail interactions. The power spectrum density (PSD) function of the track irregularity is calculated as follows:

$$S_v(\Omega) = \frac{A_v \Omega_c^2}{(\Omega^2 + \Omega_r^2)(\Omega^2 + \Omega_c^2)} \tag{7}$$

Where $S_v(\Omega)$ is the vertical power spectral density; A_v is the roughness constant (A_v=4.032×10^{-7} m^2·Rad/m); Ω_c and Ω_r are the cutoff frequency ($\Omega_c = 0.8246$ rad/m , $\Omega_r = 0.0206$ rad/m); and Ω is the spatial frequency of the irregularities. The PSD function can be transformed into vertical irregularities along the longitudinal distance of the track by means of a time-frequency transformation technique [14], as shown in Figure 6.

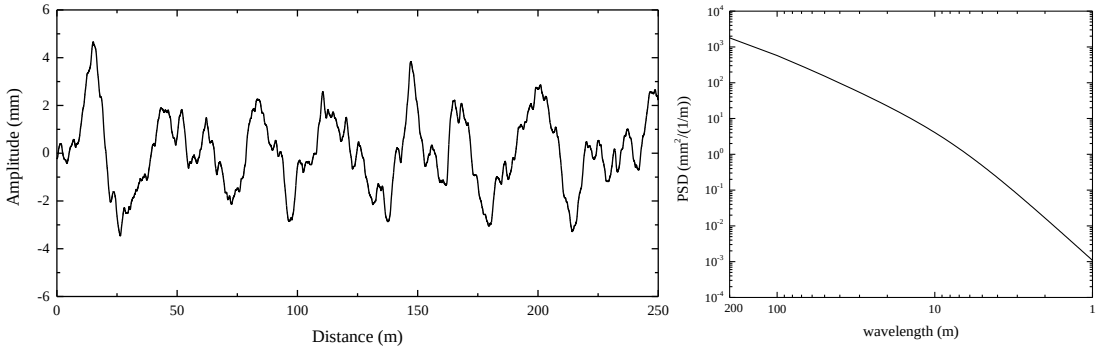

(a) (b)

Figure 6 Track irregularity (a) Track irregularity with distance (b) PSD with wavelength

3.3 Material control

When the static material properties of the slab track are used, the built-in keyword of 001-ELASTIC is used for concrete slab, CA mortar, and concrete base. The mass density, the static modulus of elasticity, and the Poisson's ratio are needed to be input by users. Also, the keywords of S01-SPRING_ELASTIC and S02-DAMPER_VISCOUS are used to describe the static stiffness and the damping of rail pads.

When the dynamic stiffness of rail pads is considered, the keywords of S01-SPRING_ELASTIC is still used but using the dynamic stiffness values for rail pads. In addition, when the strain-rate enhancement effect is considered, the keyword of 019-STRAIN_RATE_DEPENDENT_PLASTICITY is used for concrete slab, CA mortar, and concrete base. In this keyword, the yield stress and modulus of elasticity are needed as a function of the effective strain-rate. Note that the concrete and CA mortar are normally within the static stage under dynamic train loads, the yield stress of these materials can be set as a constant and high value which can protect the material from yield. The yield stress of concrete slab, CA mortar, and concrete base are set as 60 MPa, 5 MPa, and 40 MPa, respectively. As for the modulus of elasticity with effective strain-rate, it can be determined from Figure 2.

3.4 Numerical solution

The vehicle moves at a constant speed over the rail after the dynamic relaxation. The explicit central difference method is used to integrate the motion equations of the coupled vehicle and track model by LS-DYNA.

4. Model validation

The Suining-Chongqing railway in China was constructed as a test section to analyze the dynamic performance of slab tracks. Many researchers have conducted field tests to acquire the vibration responses of the vehicle and slab track [43-46]. The passenger vehicle which was running on this railway was "Changbai Mountain", which is an old vehicle type in China. Nowadays, the primary vehicle is the China Railway High-speed (CRH) 2 Electric Multiple

Unit (EMU) train, and properties of the CRH 2 EMU train are shown in Table 3 [39].

Table 3 Properties of the CRH 2 EMU train

Properties	Values
Mass of the car body (kg)	39,600
Mass of the bogie (kg)	3,500
Mass of the wheelset (kg)	2,000
Inertia of pitch motion of the car body(kg.m^2)	1.283×10^5
Inertia of pitch motion of the bogie(kg.m^2)	2,592
Stiffness of the primary suspension (N/m)	1.176×10^6
Damping of the primary suspension (N.s/m)	1.96×10^4
Stiffness of the secondary suspension (N/m)	1.89×10^6
Damping of the secondary suspension (N.s/m)	4×10^4
Length between the center of bogies (m)	17.5
Wheelbase for the bogie (m)	2.5
Radius of the wheel (m)	0.43

The field test results were recorded every time the “Changbai Mountain” or CRH 2 EMU train passes by the test section, and the train speed was 160-220 km/h. Cai and Zhai et al. [47] have conducted a numerical simulation to study the vibration responses of the slab track at 200 km/h. In their numerical model, the “Changbai Mountain” vehicle was used and the track irregularity measured from Qinhuangdao-Shenyang railway was used to excite the train-track interactions. As for the material properties of the slab track in their model, the dynamic stiffness of the rail pads and the static modulus of elasticity are used. In order to validate the simulation results calculated from the model developed in this paper, the CRH 2 EMU train and the irregularity of Germany high-speed low disturbance are adopted. Three types of material properties are considered: Case 1: using static stiffness of rail pads and static modulus of elasticity of concrete and CA mortar; Case 2: using dynamic stiffness of rail pads and static modulus of elasticity of concrete and CA mortar; Case 3: using dynamic stiffness of rail pads and dynamic modulus of elasticity of concrete and CA mortar. The vibration

responses are calculated at 200 km/h in order to compare the results with field tests and simulations. The validation results are shown in Table 4.

Table 4 Validation results

-	Field test results [43-46]	Simulation results from Cai et al [47]	Simulation results from this paper		
			Case 1	Case 2	Case 3
Wheel-rail contact force (kN)	81-116	98.7	85.4	95.3	96.3
Rail pad force (kN)	14.4-65.8	37.648	27.4	34.7	35.1
Displacement of the rail (mm)	0.3-0.88	0.827	1.243	0.878	0.863
Displacement of the slab (mm)	0.081-0.284	0.283	0.189	0.254	0.240

The field test results have a certain range for every vibration response due to the different train types and speeds and so on. The simulation results from Cai et al. [47] are within the range from field tests. Most of the simulation results from this paper in three cases are also within the range from field tests, except for the displacement of rail in case 1, in which the static material properties are used. It is also noticeable that the simulation results from this paper in all three cases are generally a little bit lower than the simulation results from Cai et al. [47]. This is mainly caused by the different track irregularities. Both PSD and amplitude of Qinhuangdao-Shenyang track irregularity are higher than the Germany low-disturbance irregularity [48], so the Qinhuangdao-Shenyang track irregularity could cause a higher excitation to train-track interactions, but the differences between two simulation models are still acceptable. Another interesting phenomenon is that there are obvious differences in vibration responses when the three types of material properties are used. These differences can be attributable to various dynamic phenomena as previously found in other dynamic track investigations [49-55]. In short, the simulation results from the model developed in this paper exhibit a good agreement with the field test results and simulation results.

5. Results and discussion

In order to highlight the influence of the dynamic material properties of the slab track on the vibration responses of train and track, the strain-rate enhancement effect for modulus of

elasticity of concrete and CA mortar under dynamic train loads is analyzed firstly. Then, the vibration responses of the vehicle, wheel-rail contact, and the track components are presented using three types of material properties: using static stiffness of rail pads and static modulus of elasticity of concrete and CA mortar (legend is named as using static properties for track components); using dynamic stiffness of rail pads and static modulus of elasticity of concrete and CA mortar (legend is named as using dynamic stiffness for rail pads); and using dynamic stiffness of rail pads and dynamic modulus of elasticity of concrete and CA mortar (legend is named as using dynamic properties for track components). And the deviation coefficients are calculated to present the effects of properties on train-track interactions.

5.1 Enhancement effects for the modulus of elasticity

The effective strain-rate is time-dependent when the vehicle is running along the track, so the dynamic moduli of elasticity of concrete and CA mortar are also time-dependent since the dynamic modulus of elasticity has the same distribution with the effective strain-rate. Figure 7 shows the contours of the distribution of the effective strain-rate of concrete slab and CA mortar when the maximum effective strain-rate occurs with the train speed of 400 km/h. The maximum effective strain-rates for concrete slab and CA mortar are 4.796×10^{-2} /s and 1.683×10^{-1} /s, respectively, and they occur at the corner of the concrete slab and CA mortar, as shown in Figure 7. Note that although the minimum effective strain-rates of concrete slab and CA mortar in Figure 7 are 2.507×10^{-4} /s and 2.082×10^{-3} /s, respectively, they are just minimum values at one moment. The actual minimum values are static effective strain rates.

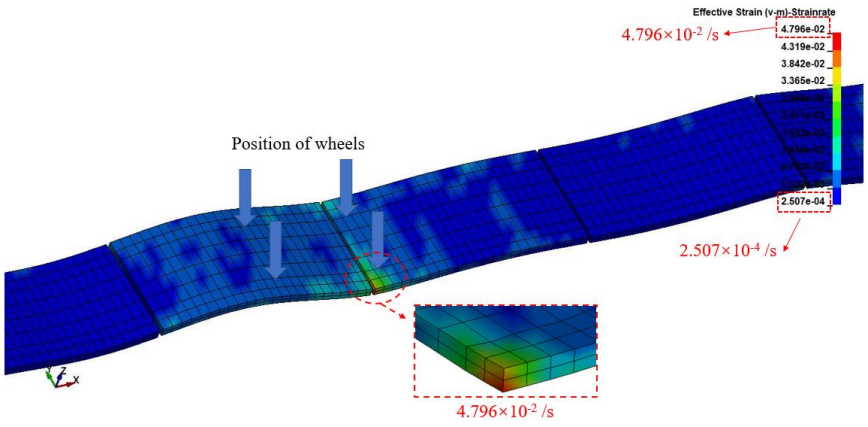

(a)

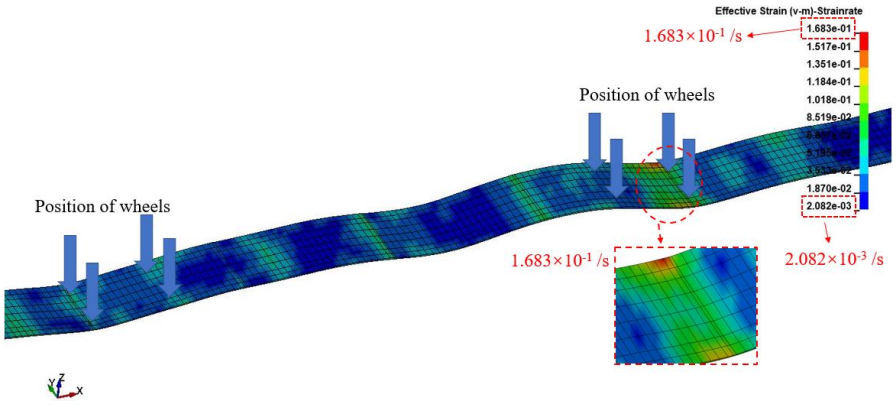

(b)

Figure 7 Contours of the effective strain-rate of the concrete slab and CA mortar at 400 km/h (a) Concrete slab (b) CA mortar (max displacement factor=3000)

The maximum and minimum effective strain-rates of concrete slab, CA mortar, and concrete base under dynamic train loads with different train speeds (from 100 km/h to 400 km/h) are shown in Table 5. When the train speed is increased, the maximum effective strain-rate is increased obviously. For concrete, the magnitude of the maximum effective strain-rate does not increase much, but the maximum effective strain-rate of CA mortar increases significantly with train speeds. As for the minimum effective strain-rate, it is within the quasi-static range and does not change much with the train speed. The minimum effective strain-rates of concrete and CA mortar at these four train speeds are 4.667×10^{-6} /s and 6.251×10^{-5} /s, respectively.

Table 5 Maximum and minimum effective strain-rates of track components under dynamic train loads

-	Train speeds	100 km/h	200 km/h	300 km/h	400 km/h
Maximum effective strain-rate (/s)	Concrete slab	1.646×10^{-2}	3.122×10^{-2}	4.021×10^{-2}	4.796×10^{-2}
	CA mortar	7.671×10^{-2}	7.457×10^{-2}	1.231×10^{-1}	1.683×10^{-1}
	Concrete base	1.206×10^{-2}	1.487×10^{-2}	3.000×10^{-2}	3.884×10^{-2}
Minimum effective strain-rate (/s)	Concrete slab	4.667×10^{-6}	9.121×10^{-6}	9.186×10^{-6}	6.054×10^{-6}
	CA mortar	9.009×10^{-5}	7.017×10^{-5}	6.251×10^{-5}	8.252×10^{-5}
	Concrete base	8.524×10^{-6}	1.479×10^{-5}	8.252×10^{-5}	1.061×10^{-5}

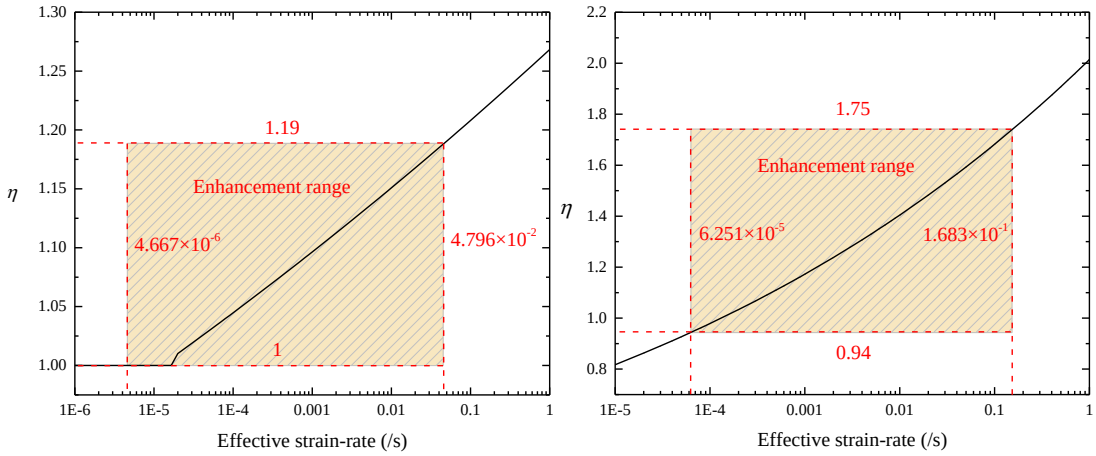

(a) (b)

Figure 8 Enhancement range (a) Concrete (b) CA mortar

The enhancement range for dynamic moduli of elasticity of concrete and CA mortar can be determined from the maximum and minimum effective strain-rate, as shown in Figure 8. Since the effective strain-rate of concrete changes from 4.667×10^{-6} /s to 4.796×10^{-2} /s, the strain-rate enhancement factor for the modulus of elasticity of concrete changes from 1 to 1.19. And for CA mortar, the strain-rate enhancement factor changes from 0.94 to 1.75. This indicates that there will be at most 19% and 75% of amplification for the moduli of elasticity of concrete and CA mortar under dynamic train loads. Also, note that although the minimum effective strain-rates of concrete and CA mortar are determined from the values at four train speeds, they are quasi-static values, indicating that these values will not change much with train speeds and can represent the minimum effective strain-rates and minimum enhancement factors.

5.2 Effects on the vibration of the vehicle

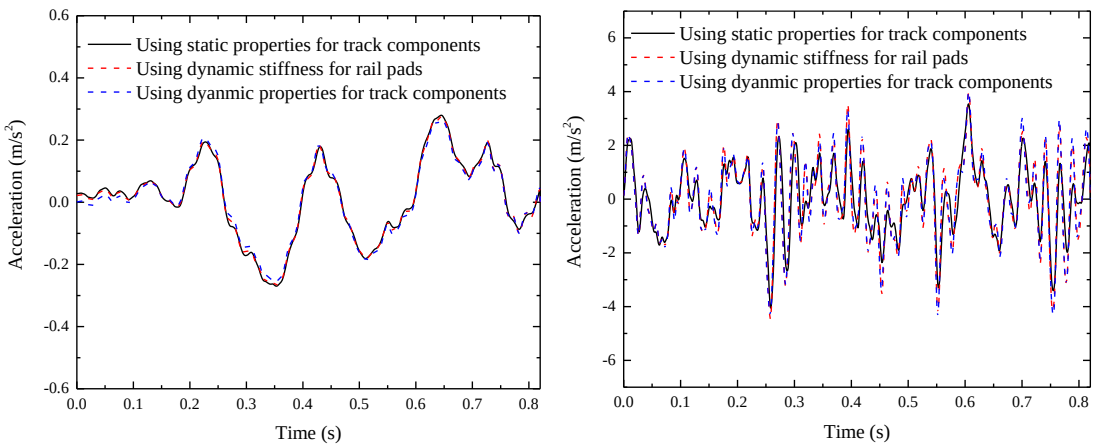

(a) (b)

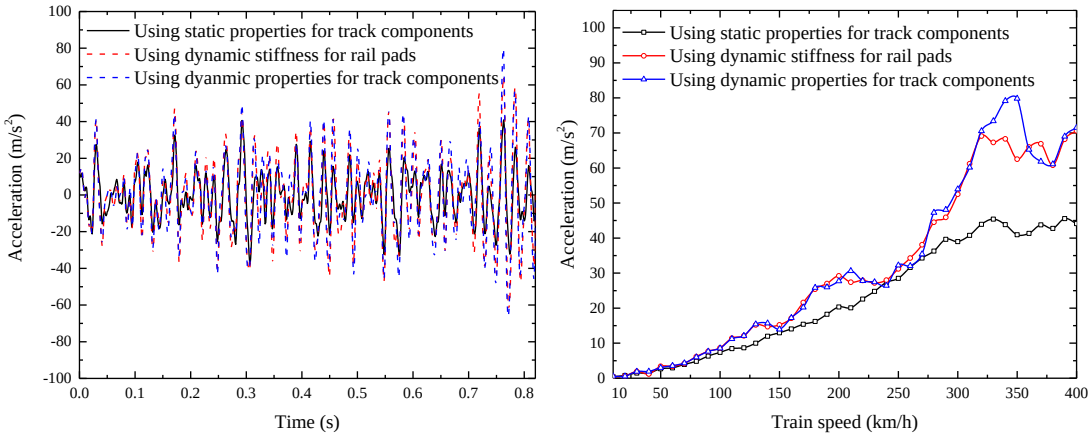

(c) (d)

Figure 9 Vertical acceleration of the vehicle (a) Time history of the acceleration of car body at 350 km/h (b) Time history of the acceleration of bogie at 350 km/h (c) Time history of the acceleration of wheelset at 350 km/h (d) Acceleration of the wheelset with train speeds

The influence of the material properties on the vibration acceleration of the vehicle is shown in Figure 9. The dynamic material properties (both dynamic stiffness and dynamic modulus of elasticity) have no significant influences on the acceleration of the car body, as shown in Figure 9 (a), but they increase the amplitudes of the acceleration of the bogie and wheelset obviously, as shown in Figure 9 (b) and (c). And there are no obvious differences in the acceleration of the bogie and wheelset whether the dynamic modulus of elasticity is used or not. Figure 9 (d) shows the relationship between the maximum acceleration of the wheelset and the train speeds. When the train speed is no more than 70 km/h, the maximum accelerations of the wheelset are quite similar either using static or dynamic material properties of slab tracks because the low train speed cannot induce significant dynamic excitation. However, once the train speed is higher than 70 km/h, the influence of the material properties on the acceleration of the wheelset can be observed. The acceleration of the wheelset is the lowest when the static material properties are used. And when the dynamic stiffness of rail pads is used, the acceleration of the wheelset is increased obviously. In addition, the influence of the dynamic modulus of the elasticity on the acceleration of the wheelset is not significant at most of the train speeds. Moreover, it seems to be two resonant peaks occurring in the acceleration of wheelset at all train speeds. One is at around 200 km/h,

and another is at around 320-360 km/h.

5.3 Effects on the wheel-rail contact force

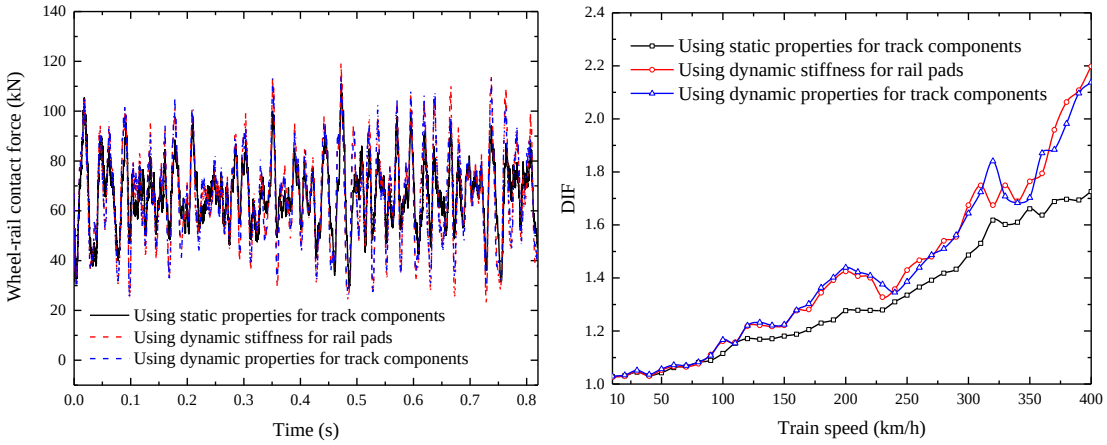

(a) (b)

Figure 10 Wheel-rail contact force (a) Time history of the wheel-rail contact force at 350 km/h (b) DIF with train speeds

It is important to calculate the dynamic impact factor (DIF) based on the wheel-rail contact force for designing the slab track in railway engineering. The DIF is calculated as follows:

$$\mathrm{DIF}=\frac{P_{\max}}{P_{\mathrm{static}}} \tag{8}$$

Where $P_{\max}$ is the maximum dynamic wheel-rail contact force, and P_{static} is the static wheel-rail contact force.

Figure 10 shows the effect of the material properties on the wheel-rail contact force. When the train speed is 350 km/h, the time history of wheel-rail contact force is shown in Figure 10 (a). The dynamic material properties (both dynamic stiffness and dynamic modulus of elasticity) could increase the amplitudes of the wheel-rail contact force, but the dynamic modulus of elasticity has no additional enlargement effect compared with the dynamic stiffness. Figure 10 (b) shows the relationship between the DIF and train speed. Similar to the acceleration of the wheelset, when the train speed is no more than 70 km/h, the material properties have no influences on the DIF. When the train speed is higher than 70 km/h, the DIF is the lowest with the static material properties. The dynamic stiffness of rail pads could

increase the DIF significantly, but the dynamic modulus of elasticity has little influences compared with the dynamic stiffness of rail pads. Also, the two resonant peaks in DIF occur at around 200 km/h and 320 km/h.

5.4 Effects on the vibration of the rail

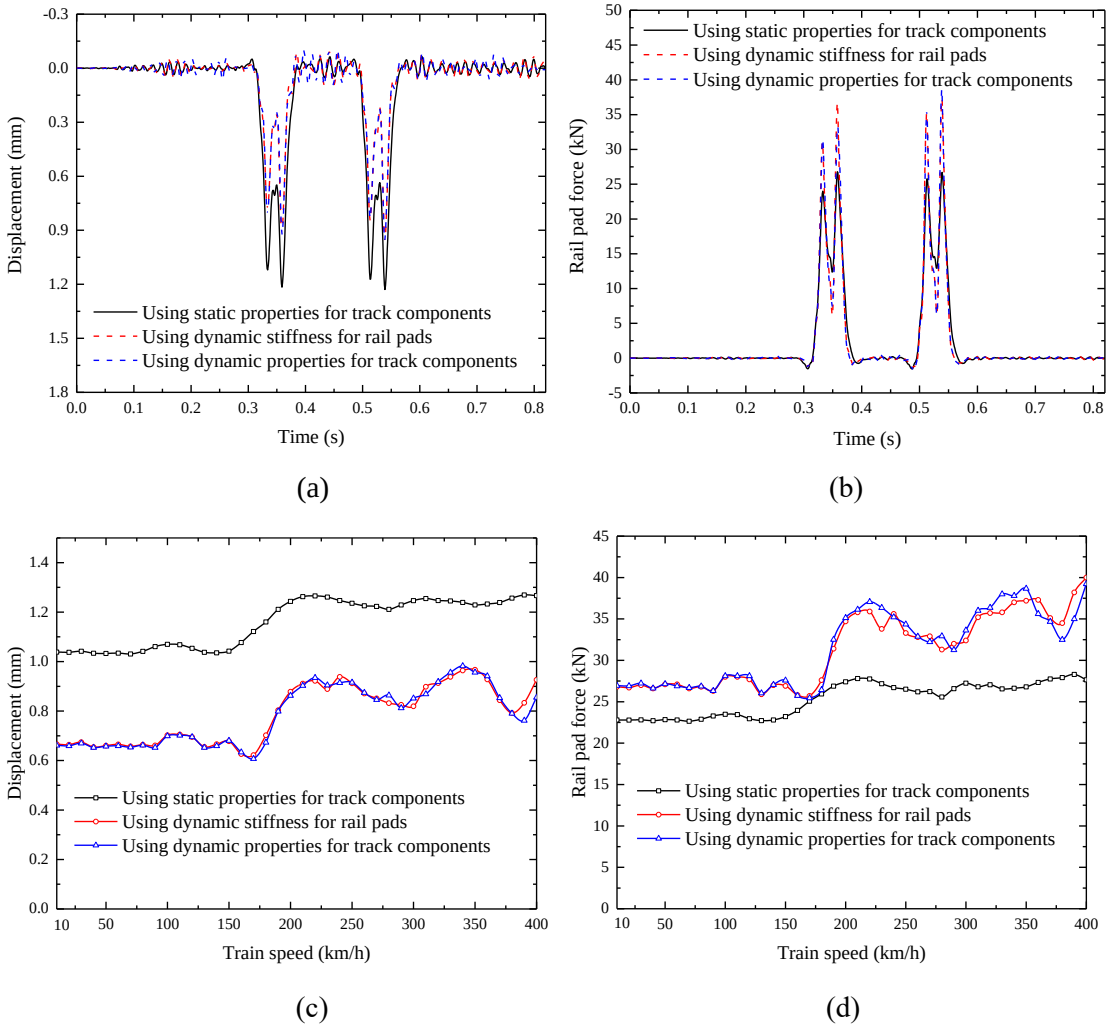

Figure 11 Dynamic responses of the rail (a) Time history of the vertical displacement of rail at 350 km/h (b) Time history of the vertical rail pad force at 350 km/h (c) Displacement of the rail with train speeds (d) Rail pad force with train speeds

Figure 11 shows the effects of the material properties on the vertical displacement of the rail and the rail pad force. When the train speed is 350 km/h, the maximum displacement of the rail using dynamic material properties is much lower than that using static properties, and the dynamic modulus of elasticity still has little influences compared with the dynamic stiffness, as shown in Figure 11(a). In contrast, the rail pad force using dynamic properties is

much higher than that using static properties, as shown in Figure 11(b). This phenomenon can also be observed at all train speeds, as shown in Figure 11 (c) and (d). And the resonant peaks using static properties seem to occur at 210 km/h and 320 km/h. When the dynamic properties are used, the peaks move to the right side at 220 km/h and 330 km/h.

5.5 Effects on the vibration of the concrete slab and CA mortar

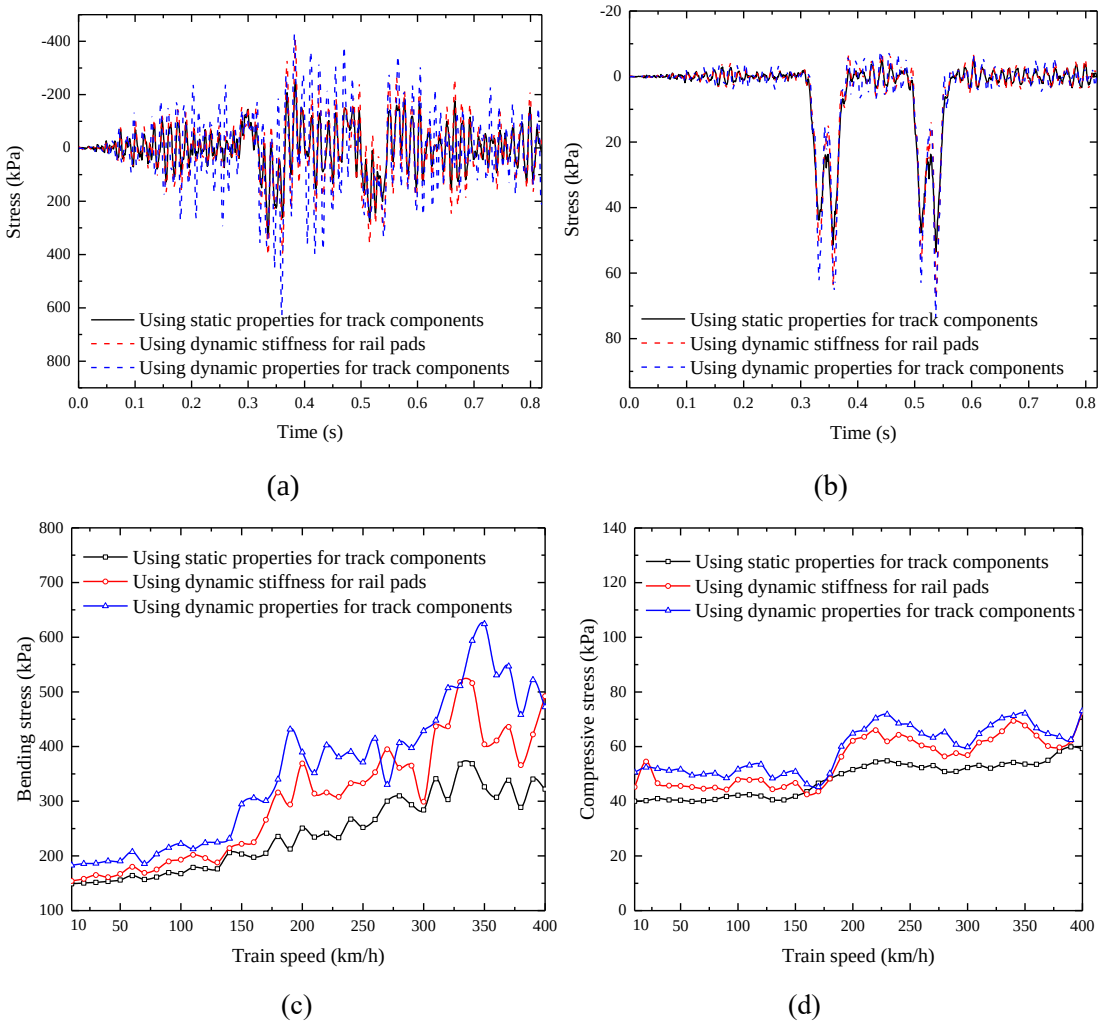

Figure 12 Dynamic stress of the slab track components (a) Time history of the bending stress of the concrete slab at 350 km/h (b) Time history of the compressive stress of the CA mortar at 350 km/h (c) Bending stress of the concrete slab with train speeds (d) Compressive stress of the CA mortar with train speeds

The concrete slab mainly undertakes bending moments under dynamic train loads. Thus the bending stress is the dominant stress for concrete slab. Also, the CA mortar mainly bears compressive loads, so that the compressive stress is the highest stress for CA mortar. When

445 the train speed is 350 km/h, the time history of the bending stress of the concrete slab and the
446 compressive stress of CA mortar with three types of material properties are shown in Figure
447 12 (a) and (b). Unlike the effect of the dynamic modulus of elasticity on the acceleration of
448 the vehicle, wheel-rail contact force, and vibration of the rail, the dynamic modulus of
449 elasticity has a significant influence on the stress of the concrete slab and CA mortar. When
450 the dynamic stiffness of rail pads is used, the maximum bending and compressive stress are
451 increased. When the dynamic modulus of elasticity is considered, the bending and
452 compressive stresses are increased furthermore. This can also be observed at all train speeds,
453 as shown in Figure 12 (c) and (d).

454 **5.6 Deviation coefficients**

455 In order to investigate the deviation of the vibration responses of the train-track
456 interactions induced by either static or dynamic material properties, the three deviation
457 coefficients are calculated as follows:

458 $$\delta_1 = \left(\frac{P_{dynamic} - P_{static}}{P_{static}} \right) \times 100\% \tag{9}$$

459 $$\delta_2 = \left(\frac{P_{dyn-stiffness} - P_{static}}{P_{static}} \right) \times 100\% \tag{10}$$

460 $$\delta_3 = \left(\frac{P_{dynamic} - P_{dyn-stiffness}}{P_{static}} \right) \times 100\% \tag{11}$$

461 Where δ_1 is the deviation coefficient which presents the deviation of vibration responses
462 induced by the dynamic stiffness of rail pads and dynamic moduli of elasticity of concrete and
463 CA mortar compared with the static material properties; δ_2 is the deviation coefficient which
464 presents the deviation of vibration responses induced by the dynamic stiffness of rail pads
465 compared with the static material properties; δ_3 is the deviation coefficient which presents the
466 deviation of vibration responses induced by the dynamic moduli of elasticity of concrete and
467 CA mortar compared with the static material properties; $P_{dynamic}$ is the maximum vibration
468 responses considering both dynamic stiffness and dynamic modulus of elasticity; P_{static} is the
469 maximum vibration responses using static material properties; and $P_{dyn-stiffness}$ is the maximum

vibration responses using dynamic stiffness for rail pads.

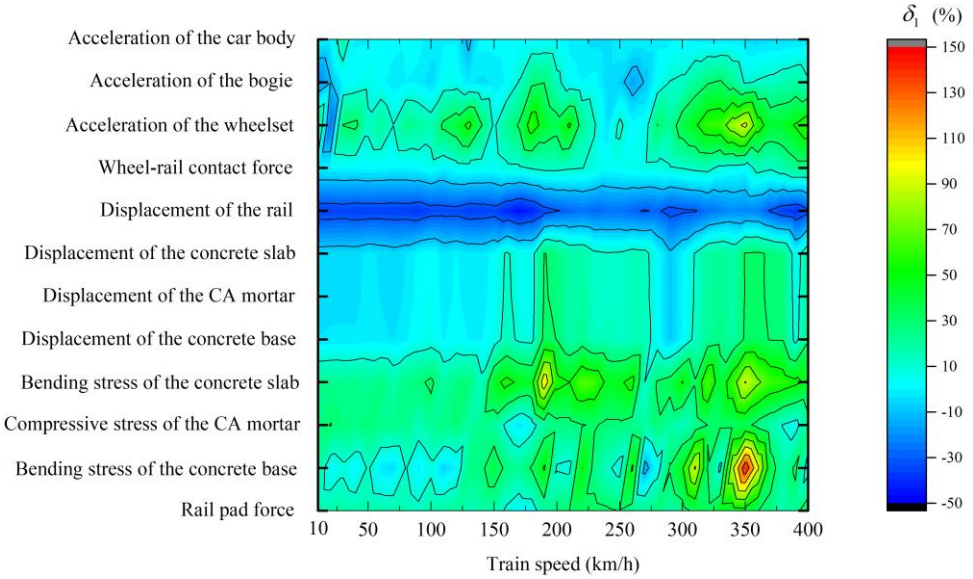

Figure 13 Contour of the deviation coefficient

Figure 13 shows the distribution of the deviation coefficient (δ_1). The maximum deviation coefficient occurs at 350 km/h in bending stress of the concrete base, and this might be induced by the resonance of the train-track interactions. The minimum deviation coefficient occurs in the displacement of the rail, which is negative because the displacement of the rail using dynamic properties is lower than that using static properties. For all of the vibration responses, the deviation coefficients are still pronounced at around 200 km/h and 350 km/h because of the resonance.

Table 6 Deviation coefficients at 350 km/h

Components	δ_1 (%)	δ_2 (%)	δ_3 (%)
Acceleration of the car body	-3.82	-1.74	-2.08
Acceleration of the bogie	8.33	9.36	-1.03
Acceleration of the wheelset	95.06	52.68	42.37
Wheel-rail contact force	2.54	6.24	-3.70
Rail pad force	44.33	38.84	5.50
Displacement of the rail	-22.19	-21.31	-0.88
Displacement of the concrete slab	30.98	30.56	0.42
Displacement of the CA mortar	30.73	30.57	0.16
Displacement of the concrete base	31.79	30.77	1.02

Bending stress of the concrete slab	91.32	23.82	67.50
Compressive stress of the CA mortar	34.67	26.33	8.34
Bending stress of the concrete base	144.36	29.89	114.47

Table 6 shows the three deviation coefficients at 350 km/h. The maximum deviation coefficient between static and dynamic material properties (δ_1) is 144.36% in the bending stress of the concrete base. The effects of the material properties on the acceleration of the wheelset and the bending stress of the slab are also pronounced since the δ_1 equals to 95.06% and 91.32%, respectively. The deviation coefficients of δ_2 are quite high on the displacement of the track components and rail pad force, indicating the dynamic stiffness of rail pads makes a significant contribution to these responses. The deviation coefficient of δ_3 accounts for a large proportion on the dynamic stress of the track components, indicating the dynamic modulus of elasticity has a significant influence on the dynamic stress of the track components.

6. Conclusions

Most train-track interaction studies have merely considered only static and quasi-static properties of materials. Despite the use of field data to tune the values of the material properties for model validations and agreements, the fundamental body of knowledge is unclear and questionable. In order to investigate the influences of the dynamic material properties on the train-track vibration interactions, the coupled vehicle-track numerical model has been developed based on the multi-body simulation principle and finite element theory in LS-DYNA with three types of material properties: static stiffness for rail pads and static moduli of elasticity for concrete and CA mortar, dynamic stiffness for rail pads and static moduli of elasticity for concrete and CA mortar, and dynamic stiffness for rail pads and strain-rate-dependent moduli for concrete and CA mortar. The model has been validated by comparing the results with the field test results and other simulations results, and a good agreement has been found. The following conclusions can be drawn:

(a) When the strain-rate-dependent moduli of elasticity of concrete and CA mortar are considered, the dynamic moduli of concrete and CA mortar are increased by at most 19% and

75% under dynamic train loads.

(b) When the train speed is no more than 70 km/h, the effect of material properties does not need to be considered for the vibration of the vehicle and wheel-rail contact force. In contrast, when the train speed is higher than 70 km/h, the dynamic material properties have a significant influence on the train-track vibration interactions.

(c) The maximum bending stress of the concrete base is increased by at most 114.36% when the dynamic material properties are used. The effect of material properties on the acceleration of the wheelset and the bending stress of concrete slab is also pronounced, although such effect on the acceleration of the car body and bogie is rather little.

(d) The stiffness of rail pads has the dominant influence on the train-track vibrations, and the dynamic modulus mainly affects the vibration stress of the track components. So the dynamic stiffness of rail pads should be considered in simulations in all cases, and the dynamic modulus of elasticity of concrete and CA mortar could be considered depends on the analysis purpose under normal track irregularities.

Acknowledgments

This research was supported by the Key Research Development Program of China (No.2016YFC0802203-2, No.2016YFC0802203-3). The authors would like to acknowledge the China Scholarship Council for the financial support. The authors sincerely thank European Commission for H2020-MSCA-RISE Project No. 691135 “RISEN: Rail Infrastructure Systems Engineering Network,” which enables a global research network that tackles the grand challenge in railway infrastructure resilience and advanced sensing under extreme conditions (www.risen2rail.eu) [56]. Technical assistance by Dr Keiichi Goto is gratefully acknowledged.

References

[1] Esveld C. Recent developments in slab track[J]. European railway review, 2003, 9(2): 81-85.

[2] Zhai W, Han Z, Chen Z, et al. Train–track–bridge dynamic interaction: a state-of-the-art review[J]. Vehicle System Dynamics, 2019: 1-44.

[3] Ren J, Deng S, Wei K, et al. Mechanical property deterioration of the prefabricated concrete slab in mixed passenger and freight railway tracks[J]. Construction and Building Materials, 2019, 208: 622-637.

[4] Li T, Su Q, Shao K, et al. Numerical Analysis of Vibration Responses in High-Speed Railways considering Mud Pumping Defect[J]. Shock and Vibration, 2019, 2019.

[5] Zhai W, Wei K, Song X, et al. Experimental investigation into ground vibrations induced by very high speed trains on a non-ballasted track[J]. Soil Dynamics and Earthquake Engineering, 2015, 72: 24-36.

[6] Zhu S, Cai C. Stress intensity factors evaluation for through-transverse crack in slab track system under vehicle dynamic load[J]. Engineering Failure Analysis, 2014, 46: 219-237.

[7] Wang M, Cai C, Zhu S, et al. Experimental study on dynamic performance of typical nonballasted track systems using a full-scale test rig[J]. Proceedings of the Institution of Mechanical Engineers, Part F: Journal of Rail and Rapid Transit, 2017, 231(4): 470-481.

[8] Lin H, Liu X, Yan H, et al. Long-Term Behavior and Performance of Ballastless Track Superstructure on China's Suining-Chongqing Railway Line[C]//2010 Joint Rail Conference. American Society of Mechanical Engineers, 2010: 299-303.

[9] Kaewunruen S, Remennikov A M. Experiments into impact behaviour of railway prestressed concrete sleepers[J]. Engineering Failure Analysis, 2011, 18(8): 2305-2315.

[10] Alexandrou G, Kouroussis G, Verlinden O. A comprehensive prediction model for vehicle/track/soil dynamic response due to wheel flats[J]. Proceedings of the Institution of Mechanical Engineers, Part F: Journal of Rail and Rapid Transit, 2016, 230(4): 1088-1104.

[11] Kaewunruen S, Remennikov A M. Field trials for dynamic characteristics of railway track and its components using impact excitation technique[J]. Ndt & E International, 2007, 40(7): 510-519.

[12] Chen X, Wu S, Zhou J. Experimental and modeling study of dynamic mechanical properties of cement paste, mortar and concrete[J]. Construction and Building Materials, 2013, 47: 419-430.

[13] Kaewunruen S, Remennikov A M. An alternative rail pad tester for measuring dynamic properties of rail pads under large preloads[J]. Experimental Mechanics, 2008, 48(1): 55-64.

[14] Tian Y, Cheng Y.R. and Liu X.W. Studies on the dynamic behaviour of U71Mn rail steel

563 under high strain rate, China Railway Science, 1992, 13, 34-42. (In Chinese).
564 [15] Bischoff P H, Perry S H. Compressive behaviour of concrete at high strain rates[J]. Materials
565 and structures, 1991, 24(6): 425-450.
566 [16] Kaewunruen S, Wang Y, Ngamkhanong C. Derailment-resistant performance of modular
567 composite rail track slabs[J]. Engineering Structures, 2018, 160: 1-11.
568 [17] Kaewunruen S, Remennikov A M. Impact capacity of railway prestressed concrete
569 sleepers[J]. Engineering Failure Analysis, 2009, 16(5): 1520-1532.
570 [18] Ngamkhanong C, Li D, Remennikov A M, et al. Dynamic capacity reduction of railway
571 prestressed concrete sleepers due to surface abrasions considering the effects of strain rate
572 and prestressing losses[J]. International Journal of Structural Stability and Dynamics, 2019,
573 19(01): 1940001.
574 [19] Xie Y, Fu Q, Zheng K, et al. Dynamic mechanical properties of cement and asphalt mortar
575 based on SHPB test[J]. Construction and Building Materials, 2014, 70: 217-225.
576 [20] Chen X, Wu S, Zhou J. Experimental and modeling study of dynamic mechanical properties
577 of cement paste, mortar and concrete[J]. Construction and Building Materials, 2013, 47:
578 419-430.
579 [21] Yongliang L, Xiangming K, Yanrong Z, et al. Static and dynamic mechanical properties of
580 cement-asphalt composites[J]. Journal of Materials in Civil Engineering, 2012, 25(10):
581 1489-1497.
582 [22] Lee O S, Kim M S. Dynamic material property characterization by using split Hopkinson
583 pressure bar (SHPB) technique[J]. Nuclear Engineering and Design, 2003, 226(2): 119-125.
584 [23] Zeng X H, Xie Y J, Deng D H, et al. A study of the dynamic mechanical properties of CRTS I
585 type CA mortar[J]. Construction and Building Materials, 2016, 112: 93-99.
586 [24] Kaewunruen S, Remennikov A M. Sensitivity analysis of free vibration characteristics of an
587 in situ railway concrete sleeper to variations of rail pad parameters[J]. Journal of Sound and
588 Vibration, 2006, 298(1-2): 453-461.
589 [25] Sol-Sánchez M, Moreno-Navarro F, Rubio-Gámez M C. The use of elastic elements in
590 railway tracks: A state of the art review[J]. Construction and building materials, 2015, 75:
591 293-305.
592 [26] Wei K, Yang Q, Dou Y, et al. Experimental investigation into temperature-and

593 frequency-dependent dynamic properties of high-speed rail pads[J]. Construction and
594 Building Materials, 2017, 151: 848-858.
595 [27] Zhai W, Wang K, Cai C. Fundamentals of vehicle–track coupled dynamics[J]. Vehicle System
596 Dynamics, 2009, 47(11): 1349-1376.
597 [28] Chen Z, Zhai W, Yin Q. Analysis of structural stresses of tracks and vehicle dynamic
598 responses in train–track–bridge system with pier settlement[J]. Proceedings of the Institution
599 of Mechanical Engineers, Part F: Journal of Rail and Rapid Transit, 2018, 232(2): 421-434.
600 [29] Xu G.H., Zhang H.P., Huang H., et al. Discussion on testing method of fastener products
601 mechanical performance of urban rail transit[J]. Shanxi Architecture,
602 2016,42(13):159-161.(In Chinese).
603 [30] CEB Bulletin Number 182, Concrete structures under impact and impulsive
604 loading-Synthesis Report; 1988.
605 [31] Birmann F. Recent investigations of the dynamic modulus of elasticity of the track in ballast
606 with regard to high speeds[M]//Railroad Track Mechanics and Technology. Pergamon, 1978:
607 197-221.
608 [32] Zhai W, Han Z, Chen Z, et al. Train–track–bridge dynamic interaction: a state-of-the-art
609 review[J]. Vehicle System Dynamics, 2019: 1-44.
610 [33] Zhu S, Cai C. Stress intensity factors evaluation for through-transverse crack in slab track
611 system under vehicle dynamic load[J]. Engineering Failure Analysis, 2014, 46: 219-237.
612 [34] Zhu S, Yang J, Yan H, et al. Low-frequency vibration control of floating slab tracks using
613 dynamic vibration absorbers[J]. Vehicle System Dynamics, 2015, 53(9): 1296-1314.
614 [35] Xu L, Zhai W. A new model for temporal–spatial stochastic analysis of vehicle–track coupled
615 systems[J]. Vehicle System Dynamics, 2017, 55(3): 427-448.
616 [36] Sun L, Chen L, Zelelew H H. Stress and deflection parametric study of high-speed railway
617 CRTS-II ballastless track slab on elevated bridge foundations[J]. Journal of Transportation
618 Engineering, 2013, 139(12): 1224-1234.
619 [37] Zhai W, Liu P, Lin J, et al. Experimental investigation on vibration behaviour of a CRH train
620 at speed of 350 km/h[J]. International Journal of Rail Transportation, 2015, 3(1): 1-16.
621 [38] Lei X, Wang J. Dynamic analysis of the train and slab track coupling system with finite
622 elements in a moving frame of reference[J]. Journal of Vibration and Control, 2014, 20(9):

623 1301-1317.
624 [39] Juanjuan R, Rongshan Y, Ping W, et al. Influence of contact loss underneath concrete
625 underlayer on dynamic performance of prefabricated concrete slab track[J]. Proceedings of
626 the Institution of Mechanical Engineers, Part F: Journal of Rail and Rapid Transit, 2017,
627 231(3): 345-358.
628 [40] Wei K, Wang F, Wang P, et al. Effect of temperature-and frequency-dependent dynamic
629 properties of rail pads on high-speed vehicle–track coupled vibrations[J]. Vehicle System
630 Dynamics, 2017, 55(3): 351-370.
631 [41] Jiang H, Chorzepa M G. An effective numerical simulation methodology to predict the
632 impact response of pre-stressed concrete members[J]. Engineering Failure Analysis, 2015, 55:
633 63-78.
634 [42] Schwer L. The Winfrith concrete model: Beauty or beast? Insights into the Winfrith concrete
635 model[C]//8th European LS-DYNA Users Conference. 2011: 23-24.
636 [43] Ren J.J., Xu J.D., Tian G.Y., et al. Field test and statistical characteristics of wheel-rail force
637 for slab track with passenger and freight traffic[J]. Engineering Mechanics,
638 2018,35(02):239-248.(In Chinese).
639 [44] Nan H.Y. Analysis on the dynamic characteristics of CRTS II type slab ballastless track on
640 subgrade and parametric study[D]. Lanzhou Jiaotong University, 2012. (In Chinese).
641 [45] Yan. S.C. Test study on subgrade load performance and the road-culvert transition
642 performance in Suiyu railway[D]. Southwest Jiaotong University, 2007.(In Chinese).
643 [46] Zhan J.X., Jiang G.L., Hu A.H., et al. Study of dynamic response of pile-plank embankment
644 of ballastless track based on field test in Suining-Chongqing High-speed Railway[J]. Rock
645 and Soil Mechanics, 2009,30(03):832-835. (In Chinese).
646 [47] Cai C.B., Zhai W.M., and Wang K.Y. Calculation and Assessment Analysis of the Dynamic
647 Performance for Slab Track on Sui-Yu Railway[J]. China Railway Science, 2006(04):17-21.
648 (In Chinese).
649 [48] Wang K.Y., Zhai W.M., and Cai C.B. Comparison on track spectra of
650 Qinhuangdao-Shenyang passenger railway line and German railway line[J]. Journal of
651 Southwest Jiaotong University, 2007(04):425-430. (In Chinese).
652 [49] Griffin D.W.P., Mirza O, Kwok K, and Kaewunruen S. Composite slabs for railway
653 construction and maintenance: a mechanistic review[J]. The IES Journal Part A: Civil &

654 Structural Engineering, 2014(7): 243-262.
655 [50] Kaewunruen S. and Remennikov A.M. An alternative rail pad tester for measuring dynamic
656 properties of rail pads under large preloads [J]. Experimental Mechanics, 2008(48): 55-64.
657 [51] Kaewunruen S. and Remennikov A.M. Current state of practice in railway track vibration
658 isolation: an Australian overview[J]. Australian Journal of Civil Engineering, 2016(14):
659 63-71.
660 [52] Kaewunruen S. and Kimani S.K. Damped frequencies of precast modular steel-concrete
661 composite railway track slabs, Steel and Composite Structures, 2017, 25 (4), 427-442
662 [53] Kimani S.K. and Kaewunruen S. Free vibrations of precast modular steel-concrete composite
663 railway track slabs, Steel and Composite Structures, 2017, 24 (1), 113-128.
664 [54] Mirza O. and Kaewunruen S. Resilience and Robustness of Composite Steel and Precast
665 Concrete Track Slabs Exposed to Train Derailments. Front. Built Environ. 2018, 4:60. doi:
666 10.3389/fbuil.2018.00060
667 [55] Kaewunruen S, Sussman JM and Einstein HH (2015) Strategic framework to achieve
668 carbon-efficient construction and maintenance of railway infrastructure systems. Front.
669 Environ. Sci. 3:6. doi: 10.3389/fenvs.2015.00006
670 [56] Kaewunruen S, Sussman JM and Matsumoto A (2016) Grand Challenges in Transportation
671 and Transit Systems. Front. Built Environ. 2:4. doi: 10.3389/fbuil.2016.00004